Photodiagnosis and Photodynamic Therapy 25 (2019) 364–368

Contents lists available at ScienceDirect

Photodiagnosis and Photodynamic Therapy

journal homepage: www.elsevier.com/locate/pdpdt

Cucurbit[7]uril enhances photosensitization of porphyrins in Neuroblastoma cells

Xiaoyu Li[a], Bo Xiao[a], Yan Guo[a], Yan Xiao[b], Song Xiao[a,*]

[a] Department of Chemistry, Guizhou Medical University, Guiyang 550025, Guizhou, China
[b] Key Laboratory of Molecular Biology, Guizhou Medical University, Guiyang 550004, Guizhou, China

ARTICLE INFO

Keywords:
PDT
Porphyrins
Cucurbit[7]uril
Phototoxicity
Photodynamic therapy

ABSTRACT

Neuroblastoma is the most common extracranial solid tumor of childhood. Advancements in treatments have improved survival rates of children suffering from this ailment. Novel therapeutic techniques may further reduce cancer related mortality. One of several emerging therapeutic options is Photodynamic Therapy (PDT) that uses light activated photosensitizer (PS) inducing cell death by apoptosis and/or necrosis. Nanotechnology has contributed to improving photosensitizers for PDT, increasing the efficiency of therapy using porphyrins and their derivatives. Efforts have been made to develop better mechanism to improve PS and consequently PDT effect. In this study, we investigated the efficacy of the PDT using porphyrins (TPOR) and TPOR/$(CB[7])_4$ (TPOR: CB[7] = 1: 4). Here we report the PDT effect of TPOR and TPOR/$(CB[7])_4$ in the treatment of the human neuroblastoma cell line (SH-SY5Y). The TPOR and TPOR/$(CB[7])_4$ didn't show more significant dark-cytotoxicity and TPOR/$(CB[7])_4$ had a stronger photodynamic effects than TPOR through generating reactive oxygen species (ROS) under irradiation with a 525 nm laser. The high photodynamic efficiency of TPOR/$(CB[7])_4$ suggests that it has the potential to be a PDT agent.

1. Introduction

Neuroblastoma is the most common extracranial solid tumor of childhood and it is responsible for 15% of pediatric cancer deaths in the United States [1]. A patient with newly diagnosed neuroblastoma can be treated with a wide range of therapies including observation only, surgery, chemotherapy, radiation, immunotherapy, differentiation therapy and autologous stem cell transplant [2]. PDT as a therapy for cancer has attracted much attention, as it has high selectivity and low toxicity, offering noninvasive clinical effectiveness and intrinsic fluorescence imaging [3–5].

PDT has three elements : photosensitizer (PS), light and oxygen [6,7].The main process of PDT is to inject a photosensitizer into the patient. After the photosensitizer accumulates in the tumor tissues, it is exposed to specific wavelength of light to produce highly ROS, particularly singlet oxygen ($^1O_2$), to destroy tumor tissues [8,9].Undoubtedly, photosensitizer is a key component in PDT. The most commonly used PSs in clinic are porphyrins and their derivates, which have some drawbacks, such as easily forming aggregates, which lead the lower efficiency of $^1O_2$ and lowering the efficiency for phototherapy [10]. Recently, nanoparticles have used to deliver PS to tumors, owing to the enhanced permeability and retention (EPR) effect [11,12].

Cucurbit[n]urils (commonly abbreviated as Q[n]s or CB[n]s) are a family of molecular container hosts bearing a rigid hydrophobic cavity and two identical carbonyl fringed portals [13].They have attracted much attention in supramolecular chemistry because of their superior molecular recognition properties in aqueous media. In particular, a recent study on the host-guest interactions of Q[*n*]s with cationic PS molecules has indicated that Q[*n*]s can significantly change the PDT efficiency of PS guests upon complexation [14].Zhang et al. have found that the Q[*n*]s plays a key role in inhibiting the aggregation of PS dyes in aqueous solution, and the resulting supramolecular interactions result in a significant antibacterial effect [15]. Marı´a Gonzalez-Bejar et al. have demonstrated that CB[7] could enhance the lifetime of the triplet excited state of PS [16].YongChao Zheng et al. have reported that CB[7] interacted with a carbazole vinylpyridinium derivative could improve the two-photon absorption and had good biocompatibility based on the host-guest inclusion interaction [17].

For the construction of the desired supramolecular photosensitizers, porphyrins are modified with four positive charges (TPOR) and CB[7] was added to the aqueous solutions of TPOR in different molar ratio. In an effort to improve PDT effects, this work describes the

* Corresponding author.
E-mail addresses: xiaoyu4621@163.com (X. Li), 735984911@qq.com (B. Xiao), 1321870045@qq.com (Y. Guo), 906503793@qq.com (Y. Xiao), xiaosong@gmc.edu.cn (S. Xiao).

https://doi.org/10.1016/j.pdpdt.2019.01.017
Received 6 November 2018; Received in revised form 7 January 2019; Accepted 11 January 2019
Available online 12 January 2019
1572-1000/

characterizations of TPOR and TPOR/$(CB[7])_4$ by fluorescence Spectroscopy and TEM. Confocal Fluorescence Microscopy was used to determine the cellular uptake of TPOR and TPOR/$(CB[7])_4$ in the SH-SY5Y cells. in vitro assays in SH-SY5Y cells showed the photodynamic efficacy of TPOR/$(CB[7])_4$ and TPOR, as determined by the MTT method and flow cytometry.

2. Materials and methods

2.1. Materials

TPOR and CB[7] were synthesized by our group, dimethyl sulfoxide (DMSO) and 1-(4,5-Dimethylthiazol-2-yl)-3,5-diphenylformazan (MTT) were purchased from Solarbio, Reactive Oxygen Species Assay Kit was bought from Sigma. Singlet Oxygen Sensor Green was bought from Invitrogen. Annexin V-FITC Apoptosis Detection Kit was bought from BD.

2.2. Cell culture

Cell line SH-SY5Y (Human Neuroblastoma Cancer) was purchased from ATCC. SH-SY5Y cells were cultured in DMED /F12 (Hyclone) medium supplemented with 10% FBS (fetal bovine serum, Gibco) and 1% penicillin/streptomycin (Hyclone). All cells were incubated at 37 °C with 5% CO_2.

2.3. Instruments

All the absorption spectra were recorded on the UV-2600 UV–vis Spectrophotometer (Shimadzu Corporation, Japan). Fluorescence spectra were recorded on the Fluorescence Spectrometer (VRIAN Cary eclipse, USA). Confocal Imaging was carried out with an OLYMPUS FV 1000 confocal laser-scanning microscope (Olympus Corporation, Japan). Ultra-microporous spectrophotometer (Biotek Epoch 2, USA). Photodynamic treatment was carried out with a laser diode (ADR-1805, 525 nm). Apotosis was analysed by Flow Cytometer (ACEA NovoCyte, USA).

2.4. Synthesis of TPOR and CB[7]

TPOR and CB[7] were synthetized using the conventional method described by Xin-Long Ni and Zhu Tao [13]. For the construction of the desired photosensitizers, the porphyrins are modified with four positive charges (TPOR) and added CB[7] to the aqueous solution of TPOR in different molar ratio. PSs were characterized by fluorescence spectroscopy.

2.5. Singlet Oxygen($^1O_2$) detection

$^1O_2$ was measured by Singlet Oxygen Sensor Green (SOSG) reagent. For $^1O_2$ generation in solution : TPOR or TPOR/$(CB[7])_4$ (10 μM) was mixed with SOSG (5 μM) in water (pH 6.5). Fluorescence measurements were made in a spectrofluorometer using excitation/emission of 488/525 nm.

2.6. The cellular localization

Cells were seeded in confocal dishes (Φ 15 mm glass bottom) and cultured overnight for attachment. Then, cells were incubated with TPOR or TPOR/$(CB[7])_4$ at concentration of 12.5 μM for 24 h. After removing the medium, cells were washed three times with PBS, and then incubated with DAPI (Solarbio, Beijing) for 30 min. Then, cells were washed with PBS for five times and imaged with a confocal laser-scanning microscope. The fluorescence of TPOR or TPOR/$(CB[7])_4$ was excited by a 546 nm laser, and the fluorescence of DAPI was excited by 488 nm laser.

2.7. ROS detection

ROS was measured by a reactive Oxygen Assay Kit using 2′,7′-dichlorodihydrofluorescein diacetate (DCFH-DA) as the fluorescence probe. For ROS measurements in cells : cells were seeded on 24-well plates (10^5 cells/well) and cultured in 5% CO_2 atmosphere at 37 °C; after cultured overnight, cells were incubated with TPOR or TPOR/$(CB[7])_4$ (12.5 μM); after cultured 24 h, cells were washed three times and incubated with DCFH-DA (10 μM) for 30 min. After washing, cells were irradiated with a 525 nm laser and the fluorescence images well collected with excitation at 488 nm and emission at 525 nm. Mean density = (IOD SUM)/(area sum), analysis by Image-Pro plus 6.0 Image Software.

2.8. Cell apoptosis assay

SH-SY5Y cells were seeded in a 6-well plate at a density of 4×10^5 cells per well and incubated with TPOR or TPOR/$(CB[7])_4$ for 24 h. After replacing the media with fresh media, the cells were irradiated under laser (95.5 mW/cm^2) for 1 min and then further incubated for 4 h. Then the cells were double-stained with 100 μl of buffer containing FITC-labeled annexin V and PI for 15 min at room temperature. Measured with NovoCyte.

2.9. In vitro cytotoxicity assay

SH-SY5Y cells were seeded in 96-well plates ($4*10^4$ cells/well) and cultured overnight for attachment.

2.9.1. Dark-toxicity study

Then TPOR or TPOR/$(CB[7])_4$ were added into cells at the concentration of 1, 2, 10, 12.5, 20 μM respectively for 24 h. The media were replaced with fresh medium (without FBS and penicillin/streptomycin) after the cells were washed three times with phosphate-buffered saline (PBS). After further incubation for 24 h, the viability of cells was measured with MTT assay.

2.9.2. Phototoxicity study

Cells were firstly incubated with TPOR or TPOR/$(CB[7])_4$ at the concentration of 12.5 μM for 24 h. After replacing the media with fresh media, the cells were irradiated under laser beam (95.5 mW/cm^2) for 30, 60, 120, 180 s respectively. The cells were continually cultured for additional 24 h, the viability of cells was measured with MTT assay.

2.10. MTT assay

The culture media of cells were replaced with 100 μL of fresh culture media containing 10% MTT reagent, and further incubated for 4 h.The absorbance at 490 nm of each well was collected with a plate reader. Cell survival rates were determined according to equation : SR = $(A - A_0) / (A_s - A_0) \times 100\%$, where A, A_s and A_0 are the absorbance of experimental group, control group without irradiation and blank group without cells.

2.11. Statistical analysis

All experiments were performed at least 3 times. Analysis was performed using GraphPad Prism 7. The one-way ANOVA test was used to compare the differences between multi groups and $p < 0.05$ was considered statistically significant.

3. Results and discussion

Analyses of the nanoparticles was performed by some techniques. Isothermal titration calorimetry experiments indicated that the binding constant (K_a) of TPOR with CB[7] was approximately 3.15×10^5 M^{-1}

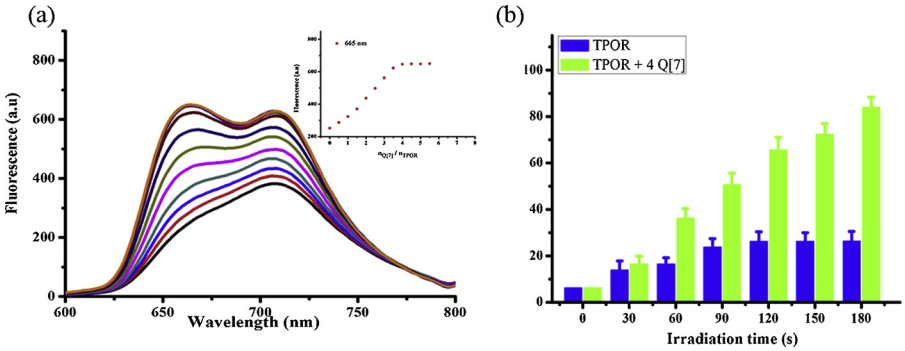

Fig. 1. (a)The fluorescence emission spectra of TPOR (C_{TPOR} = 10.0 μM) upon addition of increasing amounts (0, 0.5, 1.0, 1.5, 2.0, 2.5 3.0, 3.5, 4.0, 4.5, 5.0 equiv.) of CB[7], with an excitation of 425 nm. (b) Fluorescence intensity changes of SOSG in the presence of TPOR, TPOR/$(CB[7])_4$ and after irradiation with a 525 nm laser beam (95.5 mW/cm^2) for various time periods (C_{TPOR} = 10.0 μM, pH 6.5, saline solution, 0.3% H_2O_2).

(Fig. S1). The fluorescence spectra of TPOR upon addition of increasing amounts of CB[7] showed increased fluorescence with the fluorescence emission from 600 nm to 800 nm until the CB[7] / TPOR ratio is 4:1 and above (Fig. 1a), indicating the best ratio of CB[7] / TPOR is 4:1 and which further confirmed by transmission electron microscopy and atomic force microscopy (Fig. S2), thus suggesting that the aggregation state of TPOR was suppressed by the four bulky CB[7] molecules via noncovalent attachment to the single TPOR molecule. The porphyrins easily form aggregates based on strong hydrophobic and π-π interactions. However the aggregation state of TPOR was limited by the four bulky CB[7] noncovalent substituents via host-guest interaction, thus suppressing the quenching of their fluorescence. Interestingly, the obvious increase of the fluorescence intensity (Fig. 1a) and the molar extinction coefficient (Fig. S1) upon adding CB[7] into the TPOR aqueous solution because of the increased distance between the adjacent porphyrin chromophores leading to the suppressed self-quenching to get high quantum yield (Fig. S3) and electron microscopy observation indicated that the addition of CB[7] into solution changed the morphology of the TPOR self-assemblies. TPOR self-assembles into solid spherical-like aggregates(˜200 nm), as indicated by TEM (Fig. S2d).

Next, the ability of TPOR in the host-guest assemblies to generate $^1O_2$, which is a critical characteristic of a photosensitizer was determined. As shown in Fig. 1b, Singlet Oxygen Sensor Green (SOSG), a well-known selective $^1O_2$ fluorescent reporter, was used to determine the relative amount of singlet oxygen. Samples of TPOR and TPOR/$(CB[7])_4$ were obtained from the same samples for fluorescence determination, and all the concentrations were fixed to the same amount of TPOR guest (10.0 μM). After irradiation with a 525 nm laser beam (95.5 mW/cm^2), the samples of TPOR/$(CB[7])_4$ generated approximately 5 times more singlet oxygen than did the uncomplexed TPOR, on the basis of changes in SOSG fluorescence. The host-guest interactions of TPOR/$(CB[7])_4$ clearly enhanced the efficiency of the porphyrin cationic based PS in generating $^1O_2$ by suppressing their aggregation in aqueous solution. The TPOR/$(CB[7])_4$ appeared to have a higher $^1O_2$ generation ability than TPOR.

The activatable nature of the porphyrin cationic host-guest interaction may be suitable for imaging and PDT. To investigate these properties, the ROS generation efficiency in the excited state of the PS were further evaluated in cancer cells. Here, a cell membrane permeable organic dye, 2,7-dichlorofluorescein diacetate (DCFH-DA), was used. As an indicator of ROS generation, DCFH itself is non-emissive but is rapidly oxidized by ROS and becomes a highly fluorescent dye called dichlorofluorescein (DCF) [18,19]. The fluorescence signals from the green channel indicated the presence of DCF. As shown in Fig. 2, strong green fluorescence of DCF was observed in entire cells in the case of the TPOR/$(CB[7])_4$, thus suggesting a strong ROS-generation ability of the PSs under light irradiation. These results indicated that the host-guest interaction-based supramolecular PSs efficiently generated ROS under light excitation.

Motivated by the above results, we investigated the cellular localization and PDT efficacy of the TPOR/$(CB[7])_4$ as a PS in living cancer cells. As shown in Fig. 3a, The micrographs exhibited blue fluorescence refering to the labeling of nuclear DNA by (4′,6-diamidino-2-phenylindole) DAPI marker, while the red fluorescent dots which indicated that the TPOR and TPOR/$(CB[7])_4$ as PSs mainly localized in the cell membranes, and the much brighter red emission was observed in the group of TPOR/$(CB[7])_4$. These results indicated that TPOR/$(CB[7])_4$ efficiently entered the cells.

To determine the effects of PDT, the apoptosis of SH-SY5Y cells was detected by the flow cytometry. SH-SY5Y cells were incubated with PS and irradiated. Then the cells were stained by annexin V and PI after further incubation for 4 h. The flow cytometry results (Fig. 3b) showed that PS with out light had no significant apoptosis compared to the control. But the PDT groups had early stage of apoptosis as shown in lower right quadrants (Annexin V^+ and PI^-), especially the TPOR/$(CB[7])_4$-PDT, which had more apoptosis. These results suggested that ROS generated by photoactivated TPOR/$(CB[7])_4$ caused cell apoptosis was more efficiently.

To further demonstrate that TPOR/$(CB[7])_4$ has remarkable antitumor efficacies, we measured cell viability by MTT assay (Fig. 4). The survival rates of the cells incubated with TPOR and TPOR/$(CB[7])_4$ at a series of concentrations up to 12.5 μM for 24 h in the dark, showed no significant cell toxicity compared to control group (Fig. 4a). Upon irradiation at 525 nm and fluence 95.5 mW/cm^2 for 0, 0.5, 1, 2 and 3 min, respectively, the blank group showed no significant phototoxicity and the cell viability treated with 12.5 μM TPOR/$(CB[7])_4$ rapidly decreased to around 10% after only 1 min irradiation while the group of TPOR treatment needed 3 min (Fig. 4b). Thus, the damage to SH-SY5Y cells was from the ROS produced by the PDT light excitation process, which may be was mainly ascribed to the TPOR/$(CB[7])_4$ as the PS in the cell membranes.

Nevertheless, the effects of TPOR and TPOR/$(CB[7])_4$ have not been fully elucidated yet and the production of ROS still need to be more explored.In summary, TPOR/$(CB[7])_4$ showed excellent biocompatibility as well as greater cytotoxicity upon irradiation, suggesting that it has a potential to be used as a PDT agent in Neuroblastoma.

4. Conclusion

In summary, to design a highly effective photosensitizer, Cáceres J. et al. previously reported the encapsulation of photosensitizers including cationic porphyrin into CB[n]s (n = 7, 8) can modify their photoactivity [20], but we propose using CB[7] to enhance photosensitization in the cells have not been reported. In this work, the use of CB[7] hosts efficiently inhibited the aggregation-induced self-quenching of porphyrin cationic guests in aqueous medium. As a result, highly enhanced photosensitization was achieved. We expect that the present study will extend applications of the anticancer properties of supramolecular photosensitizers in PDT systems.

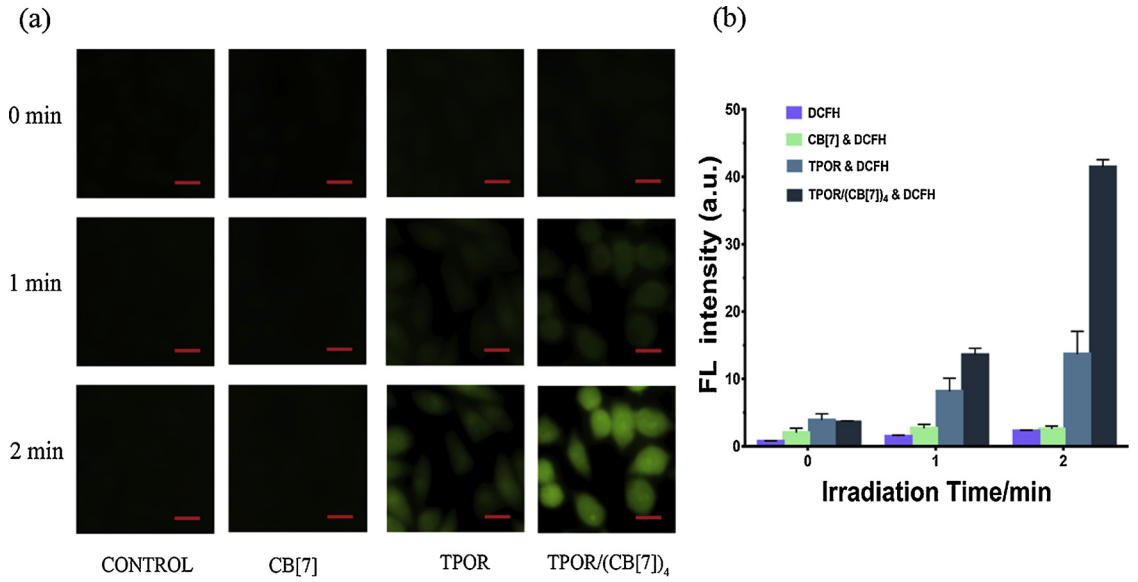

Fig. 2. ROS generation of TPOR and TPOR/$(CB[7])_4$ under irradiation in SH-SY5Y (Scale bar = 20 μm). The ROS production was determined 30 min after PDT. Data are presented as mean ± SE (n = 3).

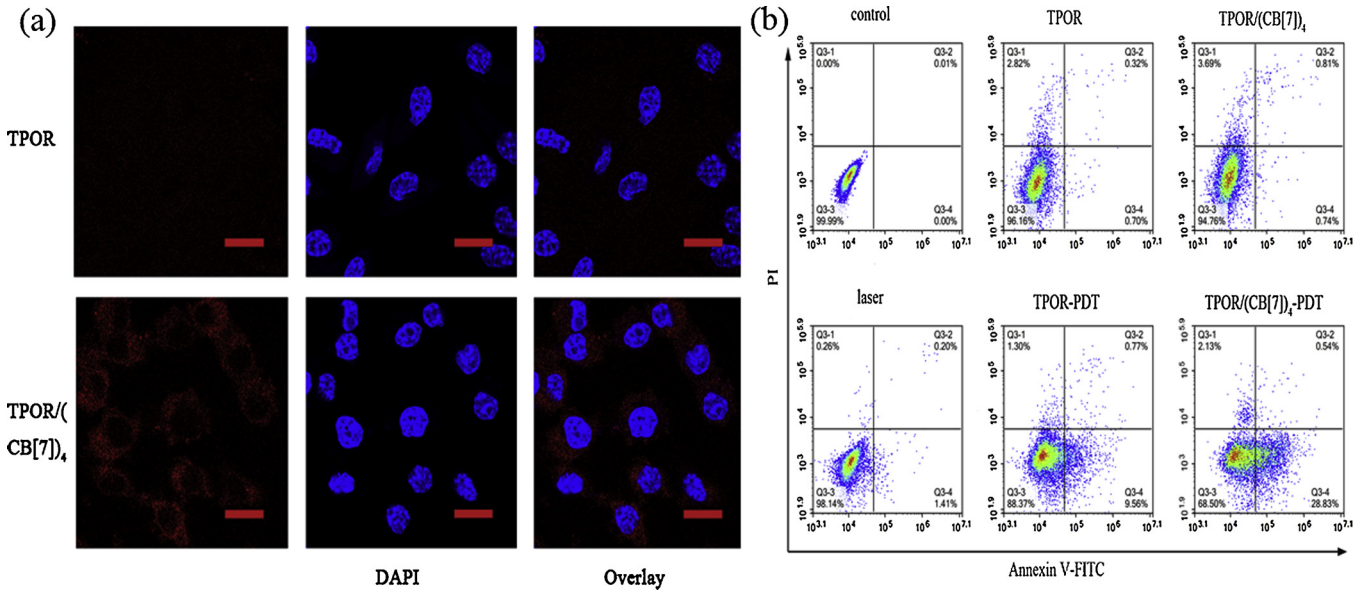

Fig. 3. a) Cellular internalization of TPOR and TPOR/$(CB[7])_4$ were conducted on SH-SY5Y cells until 24 h (Scale bar = 10 μm). b) Apoptosis rate of SH-SY5Y cells. Representative flow-cytometer of cells stained with Annexin V-FITC/PI. Control : SH-SY5Y cells without any treatment.

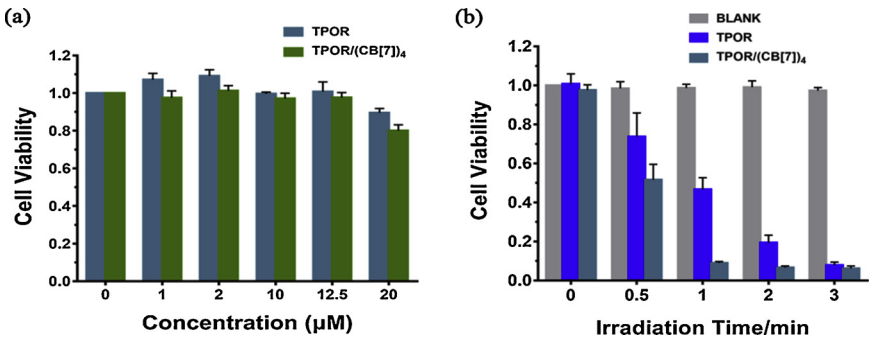

Fig. 4. The viability of SH-SY5Y measured by MTT assay after 24 h incubation time. a) Without laser irradiation. b) Upon irradiation (520 nm, 95.5 mW/cm^2). Data are presented as mean ± SE (n = 3).

Acknowledgements

This work was supported by the Natural Sciences Foundation of China (81660207) and the Science and Technology Fund of Guizhou Province (20157352)

Appendix A. Supplementary data

Supplementary material related to this article can be found, in the online version, at doi:https://doi.org/10.1016/j.pdpdt.2019.01.017.

References

[1] J.M. Maris, M.D. Hogarty, R. Bagatell, S.L. Cohn, Neuroblastoma, Lancet 369 (2007) 2106–2120.
[2] V.P. Tolbert, K.K. Matthay, Neuroblastoma: clinical and biological approach to risk stratification and treatment, Cell Tissue Res. 372 (2018) 195–209.
[3] I. Noh, D. Lee, H. Kim, C. Jeong, Y. Lee, J. Ahn, et al., Enhanced photodynamic Cancer treatment by mitochondria-targeting and brominated near-infrared fluorophores, Adv. Sci. 5 (2018) 1700481.
[4] K.K. Ng, J.F. Lovell, A. Vedadi, T. Hajian, G. Zheng, Self-assembled porphyrin nanodiscs with structure-dependent activation for phototherapy and photodiagnostic applications, ACS Nano 7 (2013) 3484–3490.
[5] P.S. Saneesh Babu, P.M. Manu, T.J. Dhanya, P. Tapas, R.N. Meera, A. Surendran, et al., Bis(3,5-diiodo-2,4,6-trihydroxyphenyl)squaraine photodynamic therapy disrupts redox homeostasis and induce mitochondria-mediated apoptosis in human breast cancer cells, Sci. Rep. UK 7 (2017) 42126.
[6] Padeliporfi N Vascular-targeted Photodynamic Therapy Versus Active Surveillance in Men With Low-risk Prostate Cancer (CLIN1001 PCM301): an Open-label, Phase 3, Randomised Controlled Trial, (2019).
[7] J. Zhang, C. Jiang, J.P. Figueiró Longo, R.B. Azevedo, H. Zhang, L.A. Muehlmann, An updated overview on the development of new photosensitizers for anticancer photodynamic therapy, Acta Pharm. Sin. B 8 (2018) 137–146.
[8] Y. Liu, X. Hu, L. Wang, X. Liu, T. Bing, W. Tan, et al., Quinacridone derivative as a new photosensitizer: photodynamic effects in cells and in vivo, Dye. Pigment. 145 (2017) 168–173.
[9] M.A. Rajora, J.W.H. Lou, G. Zheng, Advancing porphyrin's biomedical utility via supramolecular chemistry, Chem. Soc. Rev. 46 (2017) 6433–6469.
[10] Y. Hsieh, J. Zhang, W. Chuang, K. Yu, X. Huang, Y. Lee, et al., An in vitro study on the effect of combined treatment with photodynamic and chemical therapies on Candida albicans, Int. J. Mol. Sci. 19 (2018) 337.
[11] R. Riley, R. O Sullivan, A. Potocny, J. Rosenthal, E. Day, Evaluating nanoshells and a potent biladiene photosensitizer for dual photothermal and photodynamic therapy of triple negative breast cancer cells, Nanomaterials-Basel 8 (2018) 658.
[12] S. Kwiatkowski, B. Knap, D. Przystupski, J. Saczko, E. Kedzierska, K. Knap-Czop, et al., Photodynamic therapy - mechanisms, photosensitizers and combinations, Biomed. Pharmacother. 106 (2018) 1098–1107.
[13] X.L. Ni, X. Xiao, H. Cong, L.L. Liang, K. Cheng, X.J. Cheng, et al., Cucurbit[n]uril-based coordination chemistry: from simple coordination complexes to novel poly-dimensional coordination polymers, Chem. Soc. Rev. 42 (2013) 9480–9508.
[14] X. Wang, Q. Lei, J. Zhu, W. Wang, Q. Cheng, F. Gao, et al., Cucurbit[8]uril regulated activatable supramolecular photosensitizer for targeted Cancer imaging and photodynamic therapy, ACS Appl. Mater. Interfaces 8 (2016) 22892–22899.
[15] K. Liu, Y. Liu, Y. Yao, H. Yuan, S. Wang, Z. Wang, et al., Supramolecular photosensitizers with enhanced antibacterial efficiency, Angew. Chemie Int. Ed. 52 (2013) 8285–8289.
[16] M. González-Béjar, P. Montes-Navajas, H. García, J.C. Scaiano, Methylene blue encapsulation in cucurbit[7]uril: laser flash photolysis and Near-IR luminescence studies of the interaction with oxygen, Langmuir 25 (2009) 10490–10494.
[17] Y. Zheng, Y. Zhao, M. Zheng, S. Chen, J. Liu, F. Jin, et al., Cucurbit[7]uril-Carbazole two-photon photoinitiators for the fabrication of biocompatible three-dimensional hydrogel scaffolds by laser direct writing in aqueous solutions, ACS Appl. Mater. Interfaces 11 (2) (2019) 1782–1789.
[18] Z. Liu, Z. Ren, J. Zhang, C. Chuang, E. Kandaswamy, T. Zhou, et al., Role of ROS and nutritional antioxidants in human diseases, Front. Physiol. (2018) 9.
[19] B. Ghaemi, E. Shaabani, T.R. Najafi, N.S. Jafari, A. Sadeghpour, S. Kharrazi, et al., Intracellular ROS induction by Ag@ZnO core-shell nanoparticles: frontiers of permanent optically active holes in breast Cancer theranostic, ACS Appl. Mater. Interfaces 10 (29) (2018) 24370–24381.
[20] J. Caceres, J. Robinson-Duggon, A. Tapia, C. Paiva, M. Gomez, C. Bohne, et al., Photochemical behavior of biosupramolecular assemblies of photosensitizers, cucurbit[n]urils and albumins, Phys. Chem. Chem. Phys. 19 (2017) 2574–2582.